Analyst

Accepted Manuscript

This article can be cited before page numbers have been issued, to do this please use: B. Yin, Y. Tian, C. Ning, F. He and B. Ye, *Analyst*, 2018, DOI: 10.1039/C8AN01041B.

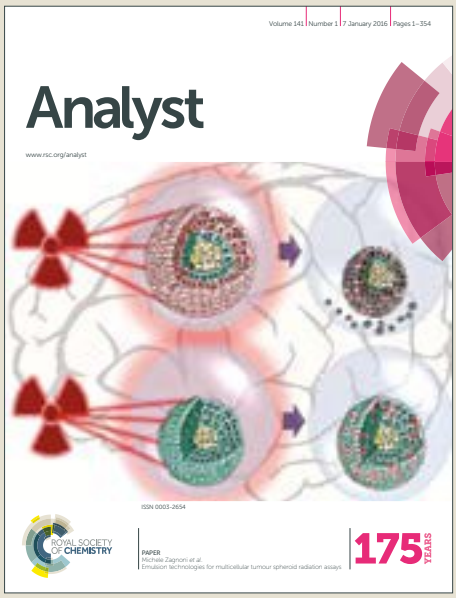

ROYAL SOCIETY OF CHEMISTRY

rsc.li/analyst

View Article Online
DOI: 10.1039/C8AN01041B

Journal Name

ARTICLE

Highly sensitive detection of exosomes by SERS using gold nanostar@Raman reporter@nanoshell structures modified with a bivalent cholesterol-labeled DNA anchor

00Received 00th January 20xx,
Accepted 00th January 20xx

DOI: 10.1039/x0xx00000x

www.rsc.org/

Ya-Fei Tian[a], Cui-Fang Ning[a], Fang He[a], Bin-Cheng Yin[*,a], and Bang-Ce Ye[*,a,b,c]

Exosomes, as important signal transmitters, play a key role in intercellular communication, especially in cancer metastasis. There is considerable evidence that exosomes can be used as an indicator of cancer. However, convenient and sensitive methods for detecting exosomes are still technically challenging. Here, we present a convenient and highly sensitive surface-enhanced Raman scattering (SERS) based method by combining immunoaffinity, SERS nanoprobes, and portable Raman devices for specific isolation and accurate quantification of exosomes. To construct the SERS-based biosensor, the surfaces of gold nanostar@4-mercaptobenzoic acid@nanoshell structures (AuNS@4-MBA@Au) are modified with a bivalent cholesterol (B-Chol)-labeled DNA anchor to prepare SERS nanoprobes. Exosomes are specifically captured by immunomagnetic beads, and then SERS nanoprobes are fixed on the surface of exosomes by hydrophobic interactions between cholesterol and lipid membranes, thus forming a sandwich-type immunocomplex. The immunocomplex can be magnetically captured and produce enhanced SERS signals. In the absence of exosomes, the sandwich-type immunocomplex can not be formed, and thus negligible SERS signals are detected. The degree of immunocomplex assembly and the corresponding SERS signals are positively correlated with the exosome concentration over a wide linear range of 40 to 4×10^7 particles/μL and the limit of detection is as low as 27 particles/μL. Consequently, a sensitive and simple strategy for detection of exosomes is successfully constructed. We believe that our biosensor has considerable potential as a convenient and highly sensitive quantification tool to detect exosomes in biological samples.

1. Introduction

Exosomes are small extracellular vesicles (30-150 nm) that are released from multivesicular bodies through an endolysosomal pathway.[1, 2] The exosomes carry abundant transmembrane and cytosolic proteins, DNA, and microRNA from parental cells,[3-5] thus serving as messengers for mediating intercellular communication.[6, 7] A great deal of evidence has demonstrated the functions of exosomes in physiological and pathological processes as intercellular communication vectors which transfer and deliver encapsulated molecules from their originating cells.[8-10] In view of their significant role in indicating disease-related, especially cancer-related, changes of the physiological state, exosomes have been recognized as candidate biomarkers for early cancer diagnosis.[5, 11-15]

At this time, exosomes are purified, usually by ultracentrifugation,[16] before quantitative analysis is performed. For the quantitative detection of exosomes, commonly used methodologies are colorimetric protein assays based on measuring the total mass of protein, but these are not very accurate because of the variable protein content in exosomes.[17] There are also other well-established methods, such as flow cytometry,[18] tunable resistive pulse sensing,[19] and nanoparticle tracking analysis for exosome quantification.[20] Many contributions have been made to the study and investigation of the exosomes by these traditional methods. However, the quantification accuracy of these methods is affected by unreliable nanoparticle counting due to interferences by lipoprotein particles and large protein aggregates. Recently, a number of novel optical methods for the detection of exosomes have been reported.[21] These new methods have achieved notable progress, such as improved sensitivity, protocols, and performance. For example, surface plasmon resonance (SPR) of ordered nanopore arrays is used to detect tumor-derived exosomes.[22] The sensitivity of this method is 4 orders of magnitude higher than that of western blotting and 2 orders of magnitude higher than that of ELISA. Zhu et al. utilized surface plasmon resonance imaging (SPRi) for quantitative detection of tumor-derived exosomes, and this method

[a]Lab of Biosystem and Microanalysis, State Key Laboratory of Bioreactor Engineering, East China University of Science and Technology, Shanghai, 200237, China
[b]Collaborative Innovation Center of Yangtze River Delta Region Green Pharmaceuticals, College of Pharmaceutical Sciences, Zhejiang University of Technology, Hangzhou 310014, Zhejiang, China
[c]School of Chemistry and Chemical Engineering, Shihezi University, Xinjiang, 832000, China
† Corresponding author: Bin-Cheng Yin, Email: binchengyin@ecust.edu.cn; Bang-Ce Ye, Email: bcye@ecust.edu.cn
†Electronic Supplementary Information (ESI) available: Details about Fig. S1-S10 and Table S1. See DOI: 10.1039/x0xx00000x

View Article Online
DOI: 10.1039/C8AN01041B

provides an easy, efficient way to detect exosomes.[23] Although these methods have led to remarkable improvements, they all rely on the customized manufacturing of precision instruments and sophisticated technical operations, which greatly limit their application range. Therefore, there is a growing need for sensitive and reliable methods to detect exosomes rapidly, especially for clinical application of exosomes as biomarkers.

In recent years, surface-enhanced Raman scattering (SERS) has attracted attention for potential applications in medical research, drug safety, and environmental monitoring.[24-26] Because the enhancement effect of SERS is mainly a result of chemical and electromagnetic field enhancement,[27] metal nanoparticles play a unique role in the amplification of Raman signals.[28, 29] SERS can depict the vibrational modes of molecules with high sensitivity,[30] and has the advantages of being label free and noninvasive, making it feasible for applications in biosensing and therapeutics.[24, 31] Although SERS analysis has been performed on many systems ranging in scale from a molecule to cell lines, few studies have focused on its application to exosomes.

In the present work, we take advantage of a specific protein (CD9) on the surfaces of exosomes and the phospholipid bilayer to develop a simple and sensitive SERS method for the quantitative detection of exosomes. The SERS-based biosensor combines immunoaffinity techniques for exosome isolation and a subsequent cholesterol-assisted membrane modification strategy for fixation of SERS nanoprobes. In the presence of exosomes, exosome are immunomagnetically captured by antibody modified magnetic beads which target CD9 proteins. SERS nanoprobes modified with bivalent cholesterol-labeled DNA strands are incorporated into the exosome membrane through hydrophobic interaction. These sandwich-type complexes can be formed between the SERS nanoprobes, exosomes and magnetic nanobeads, and can be enriched via magnetic separation. The Raman signals for SERS nanoprobes are measured for quantitative detection of exosomes. In the absence of exosomes, the magnetic complexes do not formed, and the SERS nanoprobes cannot be enriched, so only negligible SERS signals can be detected. Consequently, the proposed biosensor allows for quantitative detection of exosomes.

Experimental section

2.1 Reagents and Materials

The oligonucleotides (DNA1: 5′-SH-TTTTTTTTTTTTGCAGAAATAAGGC ACGACGGCTTT-Cholesterol-3′; DNA2: 5′-Cholesterol-TTTGCCGTCG TGCCTTATTTCTGC-3′) were synthesized by TaKaRa Biotechnology Co., Ltd. (Dalian, China). Biotin-labeled mouse anti-human CD9 antibody (anti-CD9) was purchased from QF Biosciences Co., Ltd. (Shanghai, China). Dulbecco's modified Eagle medium (DMEM), fetal bovine serum (FBS), trypsin-EDTA, and Dynabeads MyOne streptavidin magnetic beads were purchased from Thermo Fisher Scientific Co., Ltd. (Waltham, MA, USA). Hepatocellular carcinoma cell line (HepG2) was obtained from the Cell Bank of Type Culture Collection of the Chinese Academy of Sciences (Shanghai, China). ExoEasy Maxi Kit was purchased from Qiagen Translational Medicine Co., Ltd. (Suzhou, China). Hydrogen tetrachloroaurate trihydrate ($HAuCl_4 \cdot 3H_2O$), sodium citrate tribasic dihydrate ($C_6H_5Na_3O_7 \cdot 2H_2O$), silver nitrate ($AgNO_3$), L-ascorbic acid (AA), and hexadecyl trimethyl ammonium chloride (CTAC) were purchased from Aladdin (Shanghai, China). Tris(2-carboxyethy1)phosphine (TCEP) and 4-mercaptobenzoic acid (4-MBA) were purchased from Sinopharm Chemical Reagent Co. Ltd (Shanghai, China). Ten kDa filters and 0.22 μm filters were purchased from Millipore Corp. (Bedford, MA, USA). The solutions were prepared using distilled water purified by a Milli-Q water purification system (Millipore Corp., Bedford, MA, USA) with an electrical resistance of 18.2 MΩ · cm. All glassware was cleaned with freshly prepared aqua regia and rinsed thoroughly with deionized water prior to preparation of nanoparticles.

The buffers used in the procedure were: (1) phosphate buffered saline (PBS) buffer containing 8 mM Na_2HPO_4, 2 mM NaH_2PO_4, 136 mM NaCl and 2.6 mM KCl, pH 7.4; (2) washing buffer (PBST) containing 0.01% Tween-20 (v/v) in PBS buffer; (3) western blot blocking buffer (TBST) containing 20 mM Tris-HCl, pH 7.6, 150 mM NaCl, and 0.1% Tween 20; (4) electrophoresis buffer (1×TAE) containing 40 mM Tris, 20 mM acetic acid, and 1 mM EDTA, pH 8.3.

2.2 Instrumentation

Ultraviolet-visible (UV-vis) absorption spectra were recorded with a multi-detection microplate reader (Bio-Tek, Winooski, USA) using a transparent 384-well microplate. To demonstrate the overall morphology of the nanoparticles and exosomes, the samples were examined by transmission electron microscopy (TEM, JEM-1400) and high-resolution transmission electron microscopy (HRTEM, JEM-2100). The samples for TEM measurements were supported on Cu grids, and the exosomes were negatively stained with 1% phosphotungstic acid. The size distribution of the nanoparticles was measured using a Zetasizer Nano ZS system (Malvern). A 633 nm laser was used for the dynamic light scattering (DLS) characterization. The concentration and particle diameter of exosomes were measured using qNano (Izon Science Ltd., Oxford, UK). The gels were visualized under a BioRad Molecular imager (Tanon-1600, China) and Gel Image System (Tanon, China). The cells were cultured in a cell incubator (Eppendorf Galaxy 170S, Germany). Raman spectra were collected on a portable Raman spectrometer (B&W Tek Instruments, USA) equipped with a 785 nm laser, a charge-coupled device (CCD) detector and a 40× objective lens with numerical aperture (NA) 0.65. The acquisition and analysis of Raman data were performed using the BWSpec4 software. Mixing operations were conducted on a HulaMixer Sample Mixer (Thermo Fisher Scientific Co., Ltd., Waltham, MA, USA). Fetal bovine serum was ultracentrifuged using a Hitachi CP80MX with a P40ST rotor (Hitachi Aloka Medical, Tokyo, Japan).

2.3 Synthesis of AuNS@4-MBA@Au

AuNSs (60 nm) were synthesized by a seed-mediated growth method.[32] First, 100 mL of $HAuCl_4$ (1 mM) was heated to a rolling boil with vigorous stirring. Then, 15 mL of sodium citrate tribasic dihydrate (1%) was rapidly added, and the color of the solution changed from light yellow to wine red. After reacting for 15 min, the seed solution was cooled to room temperature and then stored at 4 °C. After the seed preparation, the AuNSs were fabricated. The above citrate-stabilized AuNP seed solution (200 μL) was added to 20 mL of 0.25 mM $HAuCl_4$ solution (with 20 μL of 1 M HCl) in a 50 mL centrifuge tube at room temperature. Quickly, 200 μL of $AgNO_3$ (2 mM) and 100 μL of AA (0.1 M) were added simultaneously. The solution was stirred for 30 s, and the color rapidly turned from light red to greenish-black. Then, 200 μL of SDS (2%) was added to the AuNS solution, which was left stirring for 5 min. The solution was then centrifuged at 1300 g for 15 min. The supernatant was removed and the particles were redispersed in 20 mL of distilled water. Then, 40 μL of 4-MBA (1 mM) was added to 4 mL of AuNSs

View Article Online
DOI: 10.1039/C8AN01041B

(0.1 nM) under sonication and the mixture was centrifuged 2 h later. Then, 2 mL of 0.2 M CTAC, 60 μL of 10 mM $HAuCl_4$, and 120 μL of 0.2 M AA were added to the reporter-labeled AuNS solution and stirred for 20 min.[33] Afterward, the nanoparticles were centrifuged twice at 1000 g for 20 min and redispersed in 4 mL of water.

2.4 Fabrication of B-Chol anchor-functionalized AuNS@4-MBA@Au (SERS nanoprobes)

First, 200 μL of 10 μM DNA1 was added to a 1.5 mL centrifuge tube and 10 μL of freshly prepared TCEP (10 mM) was added to the centrifuge tube to activate the thiol-modified DNA1. The solution was incubated at room temperature for 2 h. Then, 25 μL of DNA1 (10 μM) and 25 μL of DNA2 (10 μM) were prehybridized by cooling from 90 to 22 °C at a rate of 1.5 °C/min in PBS at a final concentration of 5 μM to form the bivalent cholesterol-labeled DNA anchor (B-Chol anchor). AuNS@4-MBA@Au was modified with B-Chol anchor as follows. Briefly, the B-Chol anchor (10 μL, 5 μM) was added to the as-prepared AuNS@4-MBA@Au solution (200 μL, 0.5 nM) and incubated for 3 h at room temperature. Subsequently, NaCl (10 μL, 0. 5 M) was added and then the mixture was incubated for 8 h with constant shaking. The excess DNA anchor was removed by three centrifugations at 1000 g for 15 min. The precipitate was resuspended in 100 μL of PBS buffer. The mixture was denoted as AuNS@4-MBA@Au-anchor.

2.5 Preparation of cell culture supernatant

The HepG2 cells were cultured in Dulbecco's modified essential medium (DMEM) containing 1% (v/v) penicillin-streptomycin and 10% (v/v) FBS, and maintained in a humidified atmosphere of 5% CO_2 at 37 °C. In order to reduce contamination from serum proteins and exosomes, the HepG2 cells were cultured in media which contained 10% FBS to 50% confluence, washed twice with PBS warmed to 37 °C, and then incubated for 60 h in serum-free DMEM medium. The cell culture supernatant was collected with a 50 mL centrifuge tube. Then, the supernatant was centrifuged at 480 g for 10 min to remove the intact cells and 2000 g for 15 min to remove cell debris, filtered through a 0.22 μm filter to remove large contaminating vesicles, and finally concentrated with a centrifugal device having a MWCO value of 10000.

2.6 Exosome quantification

Exosomes were isolated from cell culture supernatant using ExoEasy Maxi Kit according to the manufacturer's instructions. The concentration of exosomes was measured using qNano according to the reported literature.[34] Then, these exosomes with exact concentrations were further used as exosome standards.

2.7 Enrichment of exosome by magnetic beads

Prior to each experiment, various concentrations of exosomes were prepared using serial dilution of the above exosomes stock solution. Biotinylated CD9 antibody (anti-CD9) was immobilized on streptavidin-modified magnetic beads and used to capture exosomes. First, 10 μL of Dynabeads MyOne streptavidin magnetic beads was washed three times with PBST, and then resuspended in PBS. Two μL of 1 mg/mL biotinylated anti-CD9 was incubated with the above beads for 30 min at room temperature, followed by three washes with PBST. After washing, the anti-CD9 coupled beads were resuspended in exosomes with various concentrations (200 μL) and placed on a mixer for 10 h at 4 °C. After incubation, the beads were washed three times using PBST and used as exosome-bound beads for the following experiments.

2.8 SERS detection of exosomes

The above exosome-bound beads (200 μL) were incubated with AuNS@4-MBA@Au-anchor (100 μL, 1 nM) for 50 min at room temperature on a mixer. The resultant sandwich-type immunocomplexes were separated with a magnet and washed several times with PBST. Then, the resultant mixture was deposited on a cleaned silica slide for further SERS measurement.

3. Results and discussion

3.1 The principle of the proposed SERS-based biosensor

Scheme 1 illustrates the mechanism for exosome detection. The proposed biosensor consists of four main steps: fabrication of SERS nanoprobes, immunoaffinity capture of exosomes, linkage of SERS nanoprobes onto exosome membranes to form immunocomplexes, and SERS-based detection. First, the SERS substrate is prepared, in which reporter molecules (4-MBA) are embedded between the AuNS and Au shell. Because the strong coupling between the adjacent AuNS and Au shell, the incident electromagnetic field is squeezed into the gap, creating an enhanced local electromagnetic field and thus SERS signals. Then, two cholesterol-modified DNA single strands with complementary regions are employed to form a B-Chol anchor, which is immobilized on the surface of as-prepared AuNS@4-MBA@Au by an Au-S bond, thus forming SERS nanoprobes. Subsequently, we used a well-known exosome biomarker (CD9), which is a ubiquitous tetraspanin with various copies in the exosome surface, as a target for specific isolation of exosomes. The biotin-labeled anti-CD9 is immobilized onto the surfaces of streptavidin-linked magnetic beads for specific capture of CD9-binding exosomes. Then SERS nanoprobes can be spontaneously incorporated into the bilayer of bead-binding exosomes through hydrophobic interaction between the cholesterol moieties and the exosomal membrane, forming a sandwich-type immunocomplex. The immunocomplex can be precipitated with a magnet and thus SERS signals are detected by a Raman spectrometer. In the absence of exosomes, magnetic beads do not combine with SERS nanoprobes, after which negligible SERS signals are detected. The changes of SERS signals are positively correlated with the concentrations of exosomes, allowing quantitative detection of the target exosomes.

View Article Online
DOI: 10.1039/C8AN01041B
ARTICLE
Journal Name

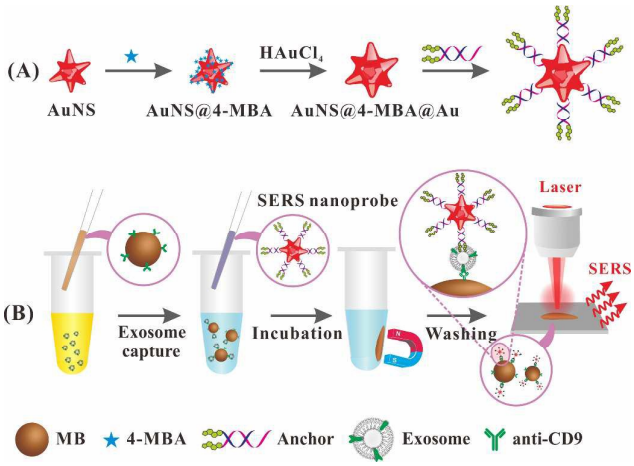

Scheme 1. Sequential SERS-based assay process for the detection of exosomes. (A) Fabrication of SERS nanoprobes (AuNS@4-MBA@Au-anchor). (B) SERS sensing strategy for exosome detection.

3.2 Synthesis and characterization of nanoparticles

The process of synthesizing nanoparticles is illustrated in Scheme 1A. AuNPs are prepared via a citrate reduction method and used as seeds for AuNS fabrication using the seed-mediated growth method. The role of $AgNO_3$ is not to form Ag branches but to assist the anisotropic growth of Au branches on certain crystallographic facets on multi-twinned citrate seeds. Au overcoated AuNS nanostructures with embedded Raman reporter molecules are prepared using 4-MBA labeled AuNS as the cores, followed by an Au overlayer growth using AA as reducing agent and CTAC as capping agent,[33] and then used for the preparation of SERS nanoprobes. TEM and UV-vis absorption spectra were used to characterize the morphological and optical changes associated with the coating process. In Fig. 1A and B, TEM images of AuNSs before and after being overcoated show the growth initiates from the AuNS core and expands outward, effectively decreasing the aspect ratio of the branches protruding from the gold core. As a result, the gold nanostar surface plasmon resonance is slightly red-shifted first from 710 nm to 725 nm after being modified with 4-MBA, and then blue-shifted down to 615 nm after the gold nanoshell coating (Fig. 1C). The colors and size distributions of the prepared nanoparticles were characterized (Fig. S1). The AuNS@4-MBA@Au can greatly enhance the Raman scattering signal (Fig. 1D), due to the locally generated "hot spots" between the gold core and shell. The stability of the as-prepared AuNS@4-MBA@ Au was investigated by observing the solution absorbance over time. As shown in Fig. S2, only slight peak broadening is observed for solution kept on the shelf for 10 days, indicating little nanoparticle aggregation. In contrast, when NaCl was added to the solution to intentionally induce aggregation, significant peak broadening and damping can be seen.

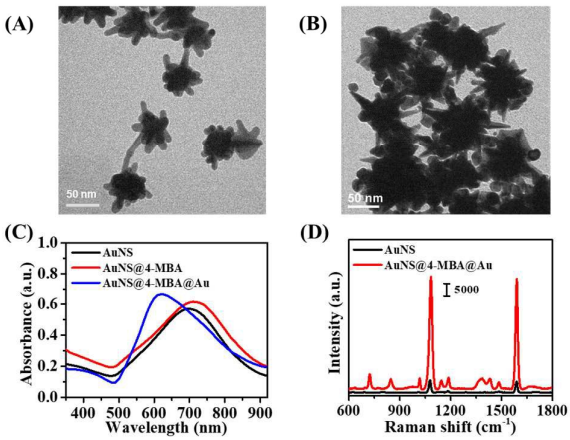

Fig. 1. TEM images of AuNS (A) and AuNS@4-MBA@Au (B); (C) UV-vis absorption spectra of the AuNS, AuNS@4-MBA, and AuNS@4-MBA@Au; (D) SERS spectra of AuNS@4-MBA and AuNS@4-MBA@Au. SERS detection parameters: $\lambda_{excitation}$ = 785 nm, accumulation time = 10 s, laser power = 100 mW.

3.3 Characterization and quantification of exosomes

Prior to exosome detection, exosomes were isolated from the cell culture supernatant of HepG2 cells by a commercial ExoEasy kit to prepare exosome standard samples. The exosomes were clearly observed by TEM (Fig. 2A). Briefly, 5 µL of exosomes was diluted with 15 µL PBS, and then adsorbed on Cu grids for 5 min. Excess exosomes were removed by filter paper. Exosomes were then negatively stained with 1% sodium phosphotungstate for 5 min. TEM images showed that the average diameter of exosomes was *ca.* 113 nm with good structural integrity. A similar size distribution of the same collected exosomes is shown in Fig. 2B by qNano characterization. For validating the efficacy of the isolation of exosomes, we analyzed CD9 and CD63 proteins by Western blotting. As shown in Fig. 2C, distinct bands of CD9 and CD63 were observed. These results were consistent with those reported in previous literatures,[23, 35] and thus the isolated exosomes were used directly for the following experiments.

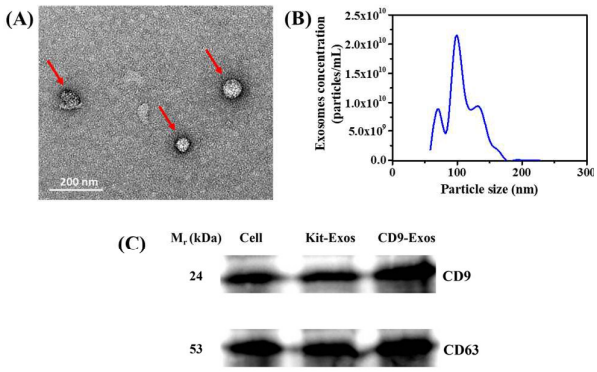

Fig. 2. Validation of exosomes purified from HepG2 cell culture supernatant. (A) TEM image of the isolated exosomes. (B) Measurement of HepG2-derived exosomes by qNano. (C) Western blotting image of CD9 and CD63 proteins from HepG2 cell lysates (cell), exosomes isolation by ExoEasy kit (Kit-Exos), and immunoaffinity capture of exosomes by magnetic beads (CD9-Exos).

View Article Online
DOI: 10.1039/C8AN01041B

3.4 Investigation of the feasibility of our biosensor

We used Raman reporter 4-MBA to investigate the feasibility of our biosensor for exosome detection. As shown in Fig. 3, in the absence of exosomes, SERS nanoprobes are not able to combine with exosome-bound beads, and cannot be assembled into a sandwich-type immunocomplex, leading to a negligible SERS signal (curve a). In the presence of different concentrations of exosomes (1×10^3 particles/μL and 1×10^4 particles/μL), SERS nanoprobes and exosome-bound beads assembled into sandwich-type immunocomplexes with many "hot spots", as demonstrated by the obvious SERS signal (curve b and c). Considering the intensity of SERS signals, we concluded that the indirect SERS sensing method using 4-MBA as Raman reporters is feasible for the detection of exosomes. In addition, the TEM image of sandwich-type immunocomplex shown in Fig. S3 further confirms the feasibility of the proposed biosensor.

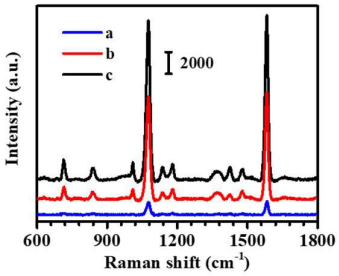

Fig. 3. SERS spectra corresponding to (a) SERS nanoprobes and exosome-bound beads in the absence of exosomes, (b) SERS nanoprobes and exosome-bound beads in the presence of 1×10^3 particles/μL and (c) 1×10^4 particles/μL exosomes. SERS detection parameters: $\lambda_{excitation}$ = 785 nm, accumulation time = 10 s, laser power = 100 mW.

3.5 Optimization of experimental conditions

The above results indicated that the proposed sensor can be used to detect exosomes. However, there will inevitably be some factors affecting the experimental results. Therefore, we studied these potential factors. The SERS active AuNS@4-MBA@Au was prepared in two steps: (1) embedding with 4-MBA, (2) coating with Au shell. Prior to the Au shell coating, we attempted to optimize the concentration of 4-MBA. First, seven different concentrations of 4-MBA ranging from 2 to 14 μM were tested, and the corresponding Raman spectra are shown in Fig. S4A. The SERS signal intensity increased as the concentration of 4-MBA increased with largest signal produced at 10 μM (Fig. S4B). Further increase in the concentration of 4-MBA resulted in a decline in signal enhancement. Thus, 10 μM of 4-MBA was chosen as the optimum concentration. After that, 4-MBA labeled AuNSs were coated with different thicknesses of Au shell and their Raman intensities were measured. Briefly, a 4-mL aliquot of the AuNS@4-MBA solution was transferred to a 10-mL centrifuge tube. After centrifugation, the precipitate was resuspended in CTAC (2 mL, 0.2 M). A concentration (varied between 50 and 500 μM) of $HAuCl_4$ and 200 μL of AA (0.2 M) were added to each solution. The color of the solution began to darken. About 20 min later, the solution color was stable, indicating that the reaction was complete. The solution was centrifuged at 1000 g for 20 min and the supernatant was removed to give a residual volume of 10 μL. Then, 10 μL of the residual solution was deposited on a cleaned silica slide for further SERS measurement. As shown in Fig. S5A, the Raman intensity of AuNS@4-MBA@Au increased noticeably as the concentration of $HAuCl_4$ varied from 50 μM to 300 μM. The maximum SERS intensity was obtained when the concentration of $HAuCl_4$ reached 300 μM. As the concentration was further increased to 500 μM, the SERS intensity dropped, which can be clearly seen in the characteristic peak at 1078 cm^{-1} (Fig. S5B). The enhanced SERS intensity may be attributed to the strong coupling between the adjacent AuNS core and Au shell, and resulting squeezing of the incident electromagnetic field into the gap, producing enhanced local electromagnetic fields and thus SERS signals.[33] Thus, 300 μM of $HAuCl_4$ was adopted as the optimum volume in the subsequent experiments.

In order to study whether the B-Chol anchor modified on the surface of AuNS@4-MBA@Au affects the SERS intensities, the SERS intensities were compared under the optimum conditions. As shown in Fig. S6, there was no change when the B-Chol anchor was modified on the surface of AuNS@4-MBA@Au, indicating that modification with the B-Chol anchor does not change the peak position in the SERS spectrum.

Finally, the incubation time for SERS nanoprobes and exosome-bound beads was investigated. As shown in Fig. S7, the SERS intensity increased rapidly as the incubation time increased from 10 to 50 min and then tended to be stable from 50 to 80 min, indicating that the interaction between SERS nanoprobes and exosomes reached equilibrium at 50 min. Thus, 50 min was chosen as the optimum incubation time in the subsequent experiments.

3.6 Sensitivity of the proposed biosensor

The sensitivity of our biosensor based on SERS was evaluated using the above optimum conditions and exosome standards in PBS. As shown in Fig. 4A, distinct SERS bands of 4-MBA at 524, 717, 845, 1011, 1078, 1144, 1178, 1412, 1480, and 1588 cm^{-1} are unambiguously observed in the presence of exosomes. The intensity of characteristic peak at 1078 cm^{-1} increases with increasing concentration of exosomes from 40 particles/μL to 4.0×10^7 particles/μL, and the SERS intensity is linearly dependent on the concentration of exosomes (Fig. 4B). The correlation equation could be expressed as $\Delta I = 3553.3 \times \lg[Exo] - 2884.8$ (R^2=0.993), in which the ΔI is defined as $I-I_0$, where I_0 and I are the SERS intensities at 1078 cm^{-1} in the absence and presence of exosomes, respectively. The limit of detection (LOD) of the biosensor was calculated to be 27 particles/μL, which is lower than the LOD of several currently available SERS methods (Table S1). Therefore, our proposed biosensor shows excellent prospects for highly sensitive analysis of exosomes.

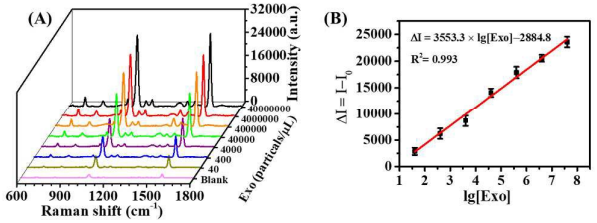

Fig. 4. (A) SERS spectra of 4-MBA for quantitative evaluation of exosomes with different concentrations. (B) Plot of change in Raman intensity at 1078 cm^{-1} *vs* the logarithm of the exosome concentration is linear over the range of 40 particles/μL-4×10^7 particles/μL. The error bars represent standard deviations based on

View Article Online
DOI: 10.1039/C8AN01041B

three independent measurements. SERS detection parameters: $\lambda_{excitation}$ = 785 nm, accumulation time = 10 s, laser power = 100 mW.

3.7 Invesitigation of reproducibility, stability, and life time of the proposed biosensor

We investigated the reproducibility of SERS signal by recording the SERS spectra of 4-MBA from 10 random spots (within an area of 60 μm^2) in the presence of 4×10^4 particles/μL exosome (Fig. S8). The SERS signal variation was less than 4.6%, indicating an excellent reproducibility of the SERS signal of the sandwich-type immunocomplex. In addition, we prepared 4 sensors of the same batch, and then applied for the detection of exosome (4×10^4 particles/μL) at different time points within 24 h to test the stability of our sensor. The results revealed that the SERS intensity could maintain 95.3% of the initial SERS intensity after 24 h (Fig. S9). The life time of our sensor was further studied. The results revealed that the SERS intensity decreased significantly from the third day (Fig. S10).

3.8 Determination of exosomes in clinical samples

In order to demonstrate the practical application of the SERS-based biosensor, human serum samples were studied. We obtained written informed consents from all participants before enrollment. All experiments were performed in accordance with the national guidelines, and approved by the ethics committee at Shanghai Changzheng Hospital. Three healthy serum sample (H1, H2, and H3) and three serum samples from liver cancer patients (P1, P2, and P3) were tested. Before the analysis, the human serum samples were centrifuged using an ultra-filter at 6300 g for 15 min. To evaluate the performance of our biosensor, we conducted a controlled trial. First, exosomes from these six serum samples were isolated by ExoEasy kit and quantified by qNano. Then, the same serum samples were assayed by our biosensor, and the exosomes were quantified using the calibration equation (Fig. 4B). As shown in Fig. 5, the results obtained from this biosensor were comparable to those obtained by the qNano method with the same serum samples. Because the CD9 is also expressed on the surfaces of non-tumorigenic cell-derived exosomes, the exosomes from healthy serum samples were also detected. However, it is noteworthy that the number of exosomes from a healthy individual is less than the number from cancer patients. Therefore, we obtained a relatively low SERS signal when exosomes from healthy serum samples were detected. The results verified previous reports that the number of exosomes is elevated in cancer patients, indicating that this phenomenon is closely related to cancer.[36]

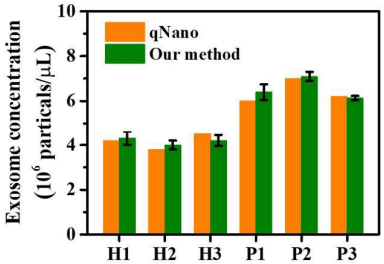

Fig. 5. Comparison of our method and ExoEasy kit coupled qNano method for the detection of exosomes in serum samples from three healthy individuals and three cancer patients.

4. Conclusions

In summary, we have developed a highly sensitive method for quantitative detection of exosomes in biological samples. In the construction of SERS biosensor, 4-MBA embedded in AuNS@Au was used as Raman reporter, B-Chol-labeled DNA anchor conjugated onto AuNS@4-MBA@Au formed SERS nanoprobes, and exosome-bound magnetic beads were used as the capture probes. Due to the SERS substrate with high activity, the sensitivity of the developed method is higher than that of the SERS methods previously reported. The SERS-based biosensor is easily fabricated, it has potential for a wide variety of applications. We believe our biosensor will be a useful platform for the analysis and quantification of exosomes in biological samples.

Acknowledgements

This work was jointly supported by the National Natural Science Foundation of China (Grants 21822402, 21335003, 21675052, 21575089), the Fundamental Research Funds for the Central Universities, the Science Fund for Creative Research Groups (Grant 21421004), and Programme of Introducing Talents of Discipline to University (Grant B16017).

Notes and references

1. S. A. Melo, H. Sugimoto, J. T. O'Connell, N. Kato A. Villanueva, A. Vidal, L. Qiu, E. Vitkin, L. T.Perelman, C. A. Melo, A. Lucci, C. Ivan, G. A. Calin and R. Kalluri, *Cancer Cell*, 2014, **26**, 707-721.
2. G. Raposo and W. Stoorvogel, *J. Cell Biol.*, 2013, **200**, 373-383.
3. L. Balaj, R. Lessard, L. Dai, Y. J. Cho, S. L. Pomeroy, X. O. Breakefield and J. Skog, *Nat. Commun.*, 2011, **2**, 180.
4. J. Skog, T. Würdinger, S. van Rijn, D. H. Meijer, L. Gainche, M. Sena-Esteves, W. T. Curry, B. S. Carter, A. M. Krichevsky and X. O. Breakefield, *Nat. Cell Biol.*, 2008, **10**, 1470-1476.
5. H. Valadi, K. Ekström, A. Bossios, M. Sjöstrand, J. J. Lee and J. O. Lötvall, *Nat. Cell Biol.*, 2007, **9**, 654-659.
6. B. N. Hannafon and W. Q. Ding, *Int. J. Mol. Sci.*, 2013, **14**, 14240-14269.
7. M. R. Speicher and K. Pantel, *Nat. Biotechnol.*, 2014, **32**, 441-454.
8. E. R. Abels and X. O. Breakefield, *Cell Mol. Neurobiol.*, 2016, **36**, 301-312.
9. T. B. Steinbichler, J. Dudas, H. Riechelmann and II. Skvortsova, *Semin. Cancer Biol.*, 2017, **44**, 170-181.
10. D. D. Taylor and C. Gercel-Taylor, *Semin. Immunopathol.*, 2011, **33**, 441-454.
11. H. Ayuko, C. S. Bruno, T. L. Shen, R. Goncalo, H. Ayako, M. M. Tesic, M. Henrik, K. Shinji, G. A. Di and C. Sophia, *Nature*, 2015, **527**, 329-335.
12. B. Costa-Silva, N. M. Aiello, A. J. Ocean, S. Singh, H. Zhang, B. K. Thakur, A. Becker, A. Hoshino, M. T. Mark, H. Molina, J. Xiang, T. Zhang, T. M. Theilen, G. Garcia-Santos, C. Williams, Y. Ararso, Y. Huang, G. Rodrigues, T. L. Shen, K. J. Labori, I. M. Lothe, E. H. Kure, J. Hernandez, A. Doussot, S. H. Ebbesen, P. M. Grandgenett, M. A. Hollingsworth, M. Jain, K. Mallya, S. K. Batra, W. R. Jarnagin, R. E. Schwartz, I.Matei, H. Peinado, B. Z. Stanger, J. Bromberg and D. Lyden, *Nat. Cell Biol.*, 2015, **17**, 816-826.
13. S. A. Melo, L. B. Luecke, C. Kahlert, A. F. Fernandez, S. T. Gammon, J. Kaye, V. S. LeBleu, E. A. Mittendorf, J. Weitz, N. Rahbari, C. Reissfelder, C. Pilarsky, M. F. Fraga, D. Piwnica-Worms and R. Kalluri, *Nature*, 2015, **523**, 177-182.

View Article Online
DOI: 10.1039/C8AN01041B

14. H. Shao, J. Chung, K. Lee, L. Balaj, C. Min, B. S. Carter, F. H. Hochberg, X. O. Breakefield, H. Lee and R. Weissleder, *Nat. Commun.*, 2015, **6**, 6999.
15. Q. Zhou, A. Rahimian, K. Son, D. S. Shin, T. Patel and A. Revzin, *Methods*, 2016, **97**, 88-93.
16. B. J. Tauro, D. W. Greening, R. A. Mathias, H. Ji, S. Mathivanan, A. M. Scott and R. J. Simpson, *Methods*, 2012, **56**, 293-304.
17. D. L. Rupert, C. Lasser, M. Eldh, S. Block, V. P. Zhdanov, J. O. Lotvall, M. Bally and F. Hook, *Anal. Chem.*, 2014, **86**, 5929-5936.
18. E. N. Nolte-'t Hoen, V. D. V. Ej, M. Aalberts, H. C. Mertens, B. J. Bosch, W. Bartelink, E. Mastrobattista, E. V. van Gaal, W. Stoorvogel and G. J. Arkesteijn, *Nanomedicine*, 2012, **8**, 712-720.
19. R. Vogel, G. Willmott, D. Kozak, G. S. Roberts, W. Anderson, L. Groenewegen, B. Glossop, A. Barnett, A. Turner and M. Trau, *Anal. Chem.*, 2011, **83**, 3499-3506.
20. W. Oosthuyzen, N. E. Sime, J. R. Ivy, E. J. Turtle, J. M. Street, J. Pound, L. E. Bath, D. J. Webb, C. D. Gregory and M. A. Bailey, *J. Physiol.*, 2013, **591**, 5833-5842.
21. d. P. E. Van, F. Coumans, Z. Varga, M. Krumrey and R. Nieuwland, *J. Thromb. Haemost.*, 2013, **11**, 36-45.
22. H. Im, H. Shao, Y. I. Park, V. M. Peterson, C. M. Castro, R. Weissleder and H. Lee, *Nat. Biotechnol.*, 2014, **32**, 490-495.
23. L. Zhu, K. Wang, J. Cui, H. Liu, X. Bu, H. Ma, W. Wang, H. Gong, C. Lausted, L. Hood, G. Yang and Z. Hu, *Anal. Chem.*, 2014, **86**, 8857-8864.
24. R. Perez-Pineiro, M. A. Correa-Duarte, V. Salgueirino and R. A. Alvarez-Puebla, *Nanoscale*, 2012, **4**, 113-116.
25. Y. Xie, Y. Li, L. Niu, H. Wang, H. Qian and W. Yao, *Talanta*, 2012, **100**, 32-37.
26. Y. Zhou, J. Chen, L. Zhang and L. Yang, *Eur. J. Inorg. Chem.*, 2012, **2012**, 3176-3182.
27. D. Graham, G. Mcanally, J. C. Jones and W. E. Smith, *Chem. Commun.*, 1998, **11**, 1187-1188.
28. S. S. Yoon, W. Lee, J. H. Byun and J. U. Lee, *J. Nanosci. Nanotechnol.*, 2015, **15**, 8996-9001.
29. R. Zhang, Y. Zhang, Z. C. Dong, S. Jiang, C. Zhang, L. G. Chen, L. Zhang, Y. Liao, J. Aizpurua and Y. Luo, *Nature*, 2013, **498**, 82-86.
30. J. Park, M. Hwang, B. Choi, H. Jeong, J. H. Jung, H. K. Kim, S. Hong, J. H. Park and Y. Choi, *Anal. Chem.*, 2017, **89**, 6695-6701. .
31. W. Ma, M. Sun, L. Xu, L. Wang, H. Kuang and C. Xu, *Chem. Commun.*, 2013, **49**, 4989-4991.
32. H. Yuan, C. G. Khoury, H. Hwang, C. M. Wilson, G. A. Grant and T. Vodinh, *Nanotechnology*,2012, **23**, 075102.
33. T. Yang and J. Jiang, *Small*, 2016, **12**, 4980-4985.
34. F. He, H. Liu, X. Guo, B.-C. Yin and B.-C. Ye, *Anal. Chem.*, 2017, **89**, 12968-12975.
35. S. Wang, L. Zhang, S. Wan, S. Cansiz, C. Cui, Y. Liu, R. Cai, C. Hong, I. T. Teng, M. Shi, Y. Wu, Y. Dong and W. Tan, *ACS Nano*, 2017, **11**, 3943-3949.
36. S. S. Kanwar, C. J. Dunlay, D. M. Simeone and S. Nagrath, *Lap. Chip.*, 2014, **14**, 1891-1900.